RESEARCH ARTICLE

Origin of an intermediate peak in DMTA analysis of multilayer ABS/PC samples

Aboubaker Alkhuder[1] | **Anne-Sophie Caro**[2] | **Matthieu Gervais**[1] | **Alain Guinault**[1] | **Patrick Ienny**[2] | **Didier Perrin**[3] | **Cyrille Sollogoub**[1]

[1]Laboratoire PIMM, CNRS, Arts et Métiers Institute of Technology, Cnam, HESAM Universite, Paris, France

[2]LMGC, IMT Mines Ales, Université Montpellier, CNRS, Alès, France

[3]Polymers Composites and Hybrids (PCH), IMT Mines Ales, Alès, France

Correspondence
Anne-Sophie Caro, LMGC, IMT Mines Ales, Université Montpellier, CNRS, 30100 Alès, France.
Email: anne-sophie.caro@mines-ales.fr

Abstract

Three layers film shaped by thermocompression of acrylonitrile butadiene styrene copolymer and polycarbonate have been analyzed in dynamic mechanical thermal analysis in tensile mode. They present two peaks as the film is loaded perpendicularly to the layers and three peaks as the film is loaded in parallel to the layers. Numerical computations confirm that the origin of this peak is not related to a mechanical issue such as the transmission of the imposed deformation from one layer to the other. Using this method, it is demonstrated that this third peak can only be obtained assuming a material transition with its own behavior between layers. Tan δ measurements provide a simple and useful experimental tool to understand more about the interfacial zone in polymer blends.

KEYWORDS

ABS/PC blends, damping, finite element method, interphase, viscoelasticity

1 | INTRODUCTION

Multiphase polymer materials (nanocomposites, polymer blends, copolymers, interpenetrating polymer networks, particulate filled polymers) have emerged as a new class of materials with enhanced properties that may be tailored to meet increasingly stringent specifications.[1] The properties of such systems depend not only on the properties of the individual components, their composition and morphology, but also on the chemical and physical interactions between the different phases.[2] In particular, the existence of an interphase, a more or less extensive area of interdiffusion or adsorption between the different components, with its own characteristic properties or property gradients, has been shown to affect the final properties of the systems: mechanical properties,[3–5] thermal transport,[6] gas barrier properties,[7] aging and degradation.[8]

Due to its small size, the interphase is quite difficult to characterize and finding a relevant tool to study its extent and properties remains still a challenge. Among the various experimental techniques used to characterize interphases (direct imaging by microscopic techniques,[9,10] reflectometry techniques either with x-rays or neutrons[11]), dynamic thermomechanical analysis (DMTA) has been proven to be an excellent probe, highly sensitive and able to give insight on the viscoelastic properties and the various relaxational mechanisms in the global systems.[12–14] In most cases, an additional damping peak was observed for multiphase polymer systems and correlated with an interphase region.[15–17] The origin of this additional peak, observed in DMTA spectra but not revealed by differential scanning calorimetry (DSC), has been widely discussed in the literature[18,19] and several explanations have been proposed: specific molecular relaxation process in the interfacial region, change in the relative moduli values of the components in the matrix-interphase-particle structure of

the blend, layer with different mechanical properties resulting from the residual thermal stresses.

An additional damping peak, located at a temperature between the glass transitions of the two components, has in particular been observed in multilayered polymer system.[20–24] While for some authors, the origin of this intermediate peak is purely mechanical, just reflecting the additive effect of the damping behavior of each phase, some others point out the importance of interfacial stress due to different thermal expansion between layers. Many efforts have been done to investigate the impact on the occurrence and amplitude of the third peak of several experimental parameters: composition ratio, number of layers, chain orientation, residual stress, cyclic, and so forth. Some contradictory results suggested that the influential parameters are highly dependent on the system studied, in particular on the compatibility between the two combined polymers, that is, the presence of an interphase, namely an interfacial layer. For example, while for polycarbonate/poly(styrene-co-acrylonitrile) (PC/SAN) multilayered systems the peak is insensitive to the number of layers,[20] its intensity is increased as the number of layers increases for more compatible systems like polypropylene/polyolefin elastomer (PP/POE),[24] propylene-ethylene copolymer/polyolefin elastomer (PPE/POE)[25] or poly(vinyl chloride)/chlorinated butyl rubber (PVC/CIIR)[26] system. Some other parameters may have an effect on the presence of the third peak such as the difference between the glass transition temperatures of the two polymers, the difference between their moduli and their temperature dependence or the coefficient of thermal expansion of both polymers. As shown by Shen et al.,[25] a two-component Takayanagi model[27] is unable to predict the apparition of the third peak suggesting that a more complete simulation is needed. Zhang et al.[28] performed a finite element analysis to simulate the distribution of shear strain in the alternating multilayer system but did not simulate the temperature dependence of the loss factor.

In this study, we aim at gaining insights on the origin of the third peak combining finite element computation and experimental characterization of the dynamic mechanical behavior of a model trilayer system. The latter is composed of acrylonitrile butadiene styrene copolymer (ABS) and polycarbonate (PC), two polymers often combined thanks to their complementary properties: heat resistance and toughness of PC (elongation at break at 50 mm/min is 125%) and ease of processability and reliable notched impact resistance of ABS (Charpy notched impact strength at 23°C is 22 kJ/m^2).[29–31] ABS and PC are known to be quite compatible since no compatibilizer is needed for ABS/PC blends.[32,33] As shown by some authors, the SAN phase of ABS interacts with the PC, leading to a good adhesion between the two polymers[33–35] and partial miscibility[36] This trilayer system is therefore of prime interest to consider the effect of an interphase and to determine its effect on the third peak.

2 | MATERIALS AND METHODS

2.1 | Materials

Terluran GP 22 Styrolution (BASF) is a very common commercial grade of ABS (MVR = 19 cm^3/10 min at 220°C with load 10 kg according to ISO 1183 test method) used for this study. Lexan PC 121R is a high fluidity polycarbonate (MFR = 21 cm^3/10 min at 300°C with load 1.2 kg according to ISO 1183) (SABIC Innovative Plastics). The relative densities and glass transition temperatures of ABS and PC are approximately 1.05 (114°C) and 1.2 (147°C) respectively.

2.2 | Preparation of blends

Trilayer systems have been realized via thermocompression with a Gibitre hot press (Italy). Films of each polymer have been prepared separately from pellets. First, polymer pellets were dried under vacuum at 80°C for 12 h before processing. Then films were pressed in the hot press with a pressure of 100 bars during 30 s at 190°C for ABS and 230°C for PC. The trilayer systems have been obtained by stacking three films (ABS/PC/ABS) and pressing them at 210°C with a pressure of 100 bars during 3 min. The thicknesses of the three stacked films have been determined in order to get a symmetric ABS/PC/ABS system with relative volume fraction of 70% ABS/30% PC (denoted respectively ϕ_{ABS}, ϕ_{PC}). The total film thickness is comprised between 3 and 4 mm.

2.3 | Characterization and methods

2.3.1 | Dynamical rheology

Dynamical mechanical thermal analysis was carried out on small bar samples under nitrogen to avoid polymer degradation and absorption of moisture using a DMTA Q800 from TA Instruments, working in dynamic tensile mode.

Samples were clamped into the DMTA in two different ways (Figure 1): in the "regular" configuration, the layers are parallel to the clamps so that the external layers of the trilayer systems, that is, ABS layers, are in

contact with the clamps. In the "orthogonal" configuration, layers are orthogonal to the clamps, so the two polymers are in contact with the clamps.

The dimensions of their microstructures are specified in Table 1.

An oscillating displacement (in the $\vec{x}$ direction, corresponding to axial strain ε_x) is applied to a sample at a given temperature, and the material response force (in the $\vec{x}$ direction, corresponding to axial stress σ_x), corresponding to this displacement, is measured.

The oscillating frequency ω was set to 1 Hz, the temperature (T) was varied from 25°C to 200°C at 2°C/min heating rate and a strain amplitude (ε_{x0}) of 0.1% was applied during the measurements, which was shown to be in the linear domain both for virgin polymers and blends.

For viscoelastic materials, the magnitude of the material response (i.e., the amplitude of force and stress) to the applied oscillating strain is shifted by a phase angle δ. From this relation between strain and stress produced in the sample, elastic storage modulus (E') and loss modulus (E'') were calculated. All measurements were reproduced twice and were well reproducible. The ratio between E'' and E' is called damping and is represented as $tan\delta$.

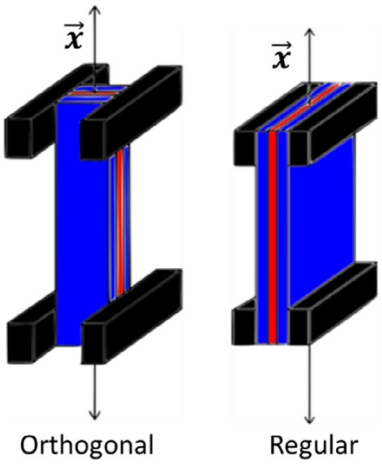

FIGURE 1 Multilayered configurations. [Color figure can be viewed at wileyonlinelibrary.com]

2.3.2 | Modeling

Methodology

Finite element (FE) modeling is an efficient tool to predict material structure properties. Numerical simulations were carried out using FE software ZeBuLon developed at Mines Paristech.[37]

Virgin polymers are expected to follow viscoelastic evolutions. At a first approximation we choose a Maxwell's model using one relaxation time τ_1 to describe their macroscopic behaviors: considering a multiaxial loading, stress $\boldsymbol{\sigma}$ and strain $\boldsymbol{\varepsilon}$ tensors are related by this relation (1):

$$\boldsymbol{\sigma}(t) = \int_0^t 2\boldsymbol{G_0} e^{-\frac{t-\tau}{\tau_1}} \dot{\boldsymbol{e}}(\tau) d\tau + \mathbf{1} \int_0^t \boldsymbol{K_0} e^{-\frac{t-\tau}{\tau_1}} tr(\dot{\boldsymbol{e}}_s) d\tau, \quad (1)$$

where the decomposition of $\boldsymbol{\varepsilon}$ in spherical $\boldsymbol{e_s}$ and deviatoric $\boldsymbol{e}$ parts is assumed as Equation (2):

$$\boldsymbol{\varepsilon}(t) = \boldsymbol{e_s}(t) + \boldsymbol{e}(t), tr(\boldsymbol{e}(t)) = \mathbf{0}, \boldsymbol{e_s}(t) = \boldsymbol{e_s}\mathbf{1}, \boldsymbol{e_s} \in \mathbb{R}. \quad (2)$$

G_0 and K_0 are instantaneous shear and bulk moduli. In expression (1) long time shear and bulk modulus are neglected. G_0 and K_0 are related to the Poisson coefficient υ via the relation (3):

$$K_0 = -\frac{2}{3}\frac{\upsilon+1}{2\upsilon-1} G_0. \quad (3)$$

In equations (1) and (2), bold letters refer to tensorial mathematical objects.

In the case of uniaxial oscillatory tensile tests, stress and strain tensors can be expressed as Equation (4):

$$\boldsymbol{\sigma}(t) = \begin{pmatrix} \sigma_x(t) & 0 & 0 \\ 0 & 0 & 0 \\ 0 & 0 & 0 \end{pmatrix}, \boldsymbol{\varepsilon}(t) = \begin{pmatrix} \varepsilon_x(t) & 0 & 0 \\ 0 & \varepsilon_y(t) & 0 \\ 0 & 0 & \varepsilon_z(t) \end{pmatrix}, \quad (4)$$

where $\varepsilon_x(t) = \varepsilon_{x0}\sin(\omega t), \varepsilon_y(t), \varepsilon_z(t)$ are the lateral and out of space strains and $\sigma_x(t) = \sigma_{0x}\sin(\omega t + \delta)$.

TABLE 1 Dimensions of the trilayer systems ABS/PC/ABS for the "orthogonal" and "regular" configurations. [Color table can be viewed at wileyonlinelibrary.com]

Geometry	ϕ_{PC}%	L (mm)	l (mm)	h (mm)	E (mm)
Orthogonal	33.5	11.88	5.02	3.42	1.68
Regular	33.3	15.50	3.42	5.02	1.14

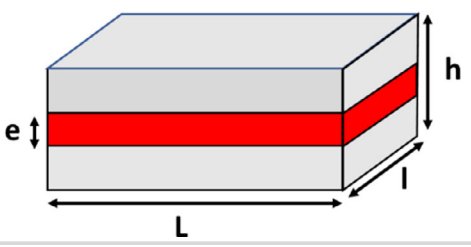

Assuming ε_{x0}, material parameters τ_1, υ and G_0 known, σ_{0x} and δ can be deduced from a FE simulation. Only one finite element is used for this latest simulation as the simulation corresponds to a homogeneous test and classical boundary conditions of a uniaxial tensile test are applied. As a sinusoidal strain signal (amplitude ε_{x0}, frequency ω) is applied, the analysis of stress signal after numerical simulation enables the determination of σ_{0x} and δ.

Identification of material parameters of virgin polymers

DMTA experiments are able to evaluate the evolution of $E'(T)$, $E''(T)$, and thus $tan\delta(T)$ versus temperature for neat polymers.

From $\delta(T)$ and $E'(T)$, the evaluation of stress magnitude σ_{0x} is available for each testing temperature via the relation (5):

$$\sigma_{0x}(T) = \frac{\varepsilon_{0x} E'(T)}{cos\delta(T)}. \tag{5}$$

As rheological behavior of each polymer is strongly dependent of temperature, it is assumed by that way that virgin polymer behavior can be described via the knowledge of three parameters τ_1, υ and G_0, strongly dependent on temperature.

The optimum material parameters (τ_1, υ, G_0) correspond to the best accordance between experimental and numerical strain amplitude and phase shift.

To solve this non-linear problem, an optimization scheme, based on sequential quadratic programming (SQP) algorithm, is selected. This second order local optimizer is included in the optimisation module "Z-optim" of ZeBuLon's software. The gap between experimental and numerical stress values σ_{0x} and δ at each temperature T is computed via a cost function written as follows:

$$J(\tau_1, \upsilon, G_0) = \frac{1}{2}\left(\sigma_{0x}(\tau_1, \upsilon, G_0) - \sigma_{0x\,exp}\right)^2 + \left(\delta(\tau_1, \upsilon, G_0) - \delta_{exp}\right)^2. \tag{6}$$

The problem is thus to solve, at each temperature following Equation (7):

$$Inf_{(\tau_1, \upsilon, G_0) \in \mathbb{R}^3} J(\tau_1, \upsilon, G_0). \tag{7}$$

Prediction of multilayered behavior

A quarter of the geometry of the trilayer model system is considered thanks to the symmetries of the geometry and boundary conditions Geometry and meshes are presented in Figure 2. In FE simulations displacement continuity is assumed at the interface ABS/PC. Materials properties of ABS and PC, for each temperature, are defined through preliminary simulations (see section 2.3.2.2). The volumes are subjected to displacement values $\boldsymbol{h\varepsilon_{0x} sin(\omega t)}$ on lateral surfaces delimitated by the dotted rectangle (height of 2 mm) on Figure 2. $\boldsymbol{E'(T)}$, $\boldsymbol{E''(T)}$ and thus $\boldsymbol{\tan\delta(T)}$ of the multilayered materials can therefore be obtained and compared to the experimental ones.

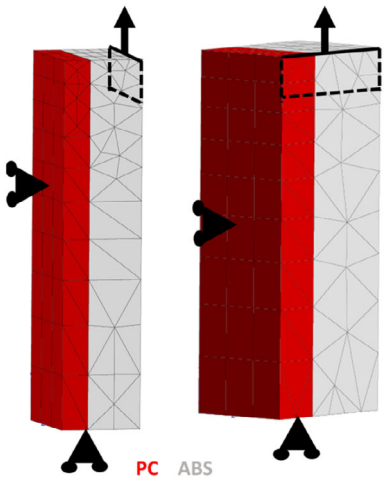

FIGURE 2 FE geometries and meshes, "regular" (left) "orthogonal" (right) configuration. [Color figure can be viewed at wileyonlinelibrary.com]

3 | RESULTS AND DISCUSSION

3.1 | Rheological properties

3.1.1 | Virgin polymers

Figure 3 presents the evolution of E' and $\tan\delta$ as a function of temperature for ABS and PC polymers obtained with DMTA equipment. Both polymers exhibit one transition peak corresponding to the glass transition temperature of the amorphous polymers, located at 114°C and 147°C for ABS and PC respectively. As expected, the storage moduli show a pronounced decrease of two to three decades after the glass transitions.

3.1.2 | Multilayered structure behavior

Results of the dynamic mechanical analysis of the multilayered materials are presented in Figure 4. In both "orthogonal" and "regular" configurations, native damping peaks of PC and ABS are visible, which is clearly an

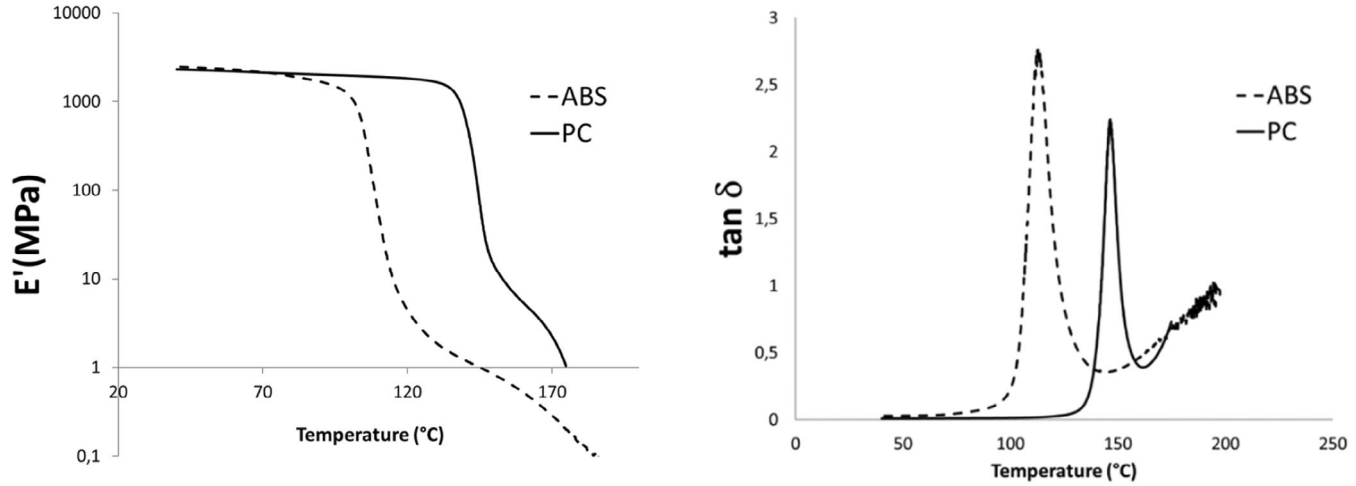

FIGURE 3 Evolution of storage moduli (left) and loss tangent moduli (right) of neat polymer acrylonitrile butadiene styrene copolymer (ABS) and polycarbonate (PC) versus temperature.

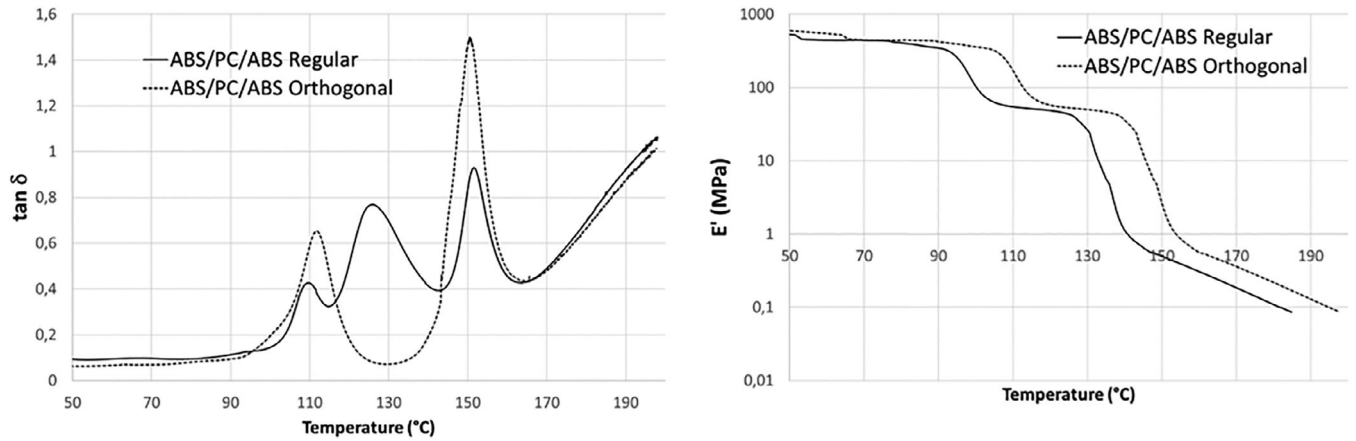

FIGURE 4 Effect of the orientation of the sample in dynamic thermomechanical analysis (DMTA) apparatus on the intermediate peak (left) and on the storage modulus (right) for acrylonitrile butadiene styrene copolymer (ABS)/polycarbonate (PC)/ABS three-layer samples.

indication of PC and ABS immiscibility. As expected, the storage modulus decreases with temperature for both configurations while shifted for the "orthogonal" configuration.

Moreover the "regular" multilayer structure leads to the presence of an additional intermediate damping peak. As discussed in the introduction, the origin of this intermediate peak is still debated. The fact that this third peak is measured only for "regular" configuration would suggest that its origin is rather purely mechanical and reflects the additive effect of the damping behavior of ABS and PC. Moreover, the contribution of the residual stresses[38] and their progressive relaxation in temperature should be involved. Modeling approach was used to shed new light on the origin of this peak.

3.2 | Modeling

3.2.1 | Virgin polymers

The first step was to define materials properties (τ_1, υ, G_0) of ABS and PC depending on temperatures. The methodology used is the one presented in section 2.3.2.2. The discrete temperatures are chosen to correspond to critical points of $E'(T)$ and tan $\delta(T)$:

$$T \epsilon \{100, 108, 110, 113, 117, 120, 125, 130, 135, 140, 143, 147, 150, 155, 160^{\circ}C\}.$$

The Poisson's ratio of viscoelastic materials cannot be regarded as a constant parameter, but as a time-

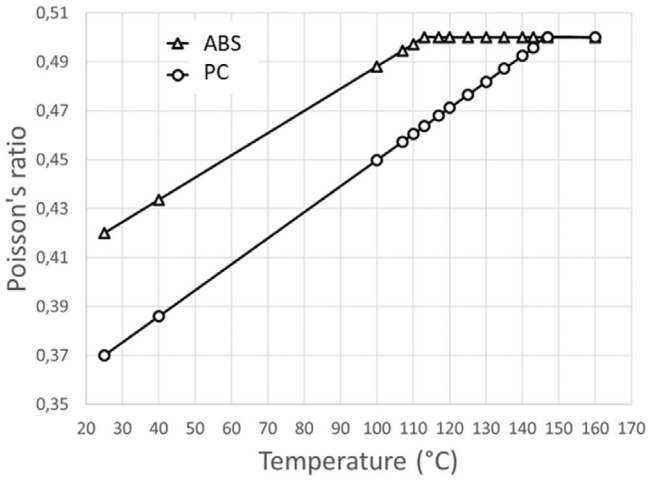

FIGURE 5 Poisson's ratio of polycarbonate (PC) and acrylonitrile butadiene styrene copolymer (ABS) versus temperature–trend curves (solid line).

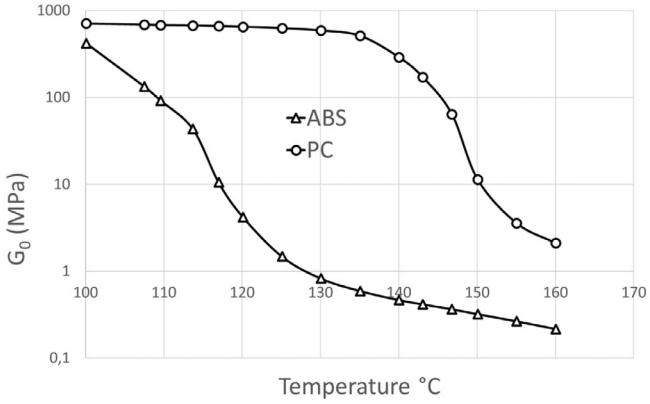

FIGURE 6 Instantaneous shear modulus versus temperature—zoom on temperatures between 100 and 160°C—trend curves (solid line).

dependent material function, being increased according to the temperature. Some authors found that this dependence can be fitted with a sigmoidal function, extending from a lower plateau value to an upper plateau value scattered around 0.5.[39,40] For the sake of simplicity, we assume a bilinear evolution for the Poisson's ratio from the value given in the data sheet ($\upsilon_{PC} = 0.37$, $\upsilon_{ABS} = 0.42$ at 25°C) to 0.5 around glass transition (see Figure 5).

The algorithm of minimization quickly converges toward a solution for each polymer and each temperature. (τ_1, G_0) are presented in Figure 6 and Figure 7 (left) for the temperatures between 100 and 160°C, stages of maximum variabilities for these variables. These material parameters lead to an accurate description of $\tan\delta(T)$ curve (see dot points corresponding to this minimization on the graph of Figure 8 [right]).

3.2.2 | Multilayered materials

Numerical computations are conducted through 3D simulations as described in section 2.3.2.2.

Comparison between loss factors related to "orthogonal" and "regular" loadings is given in Figure 8. As expected, the loss factor peaks of native polymers are clearly present even if for the "orthogonal" simulation, the one of ABS is slightly shifted toward the lower temperatures. Moreover, for the "regular" configuration, ABS layer does not transmit the load as it shows a low elastic modulus, in comparison to PC. In both configurations, layers are not subjected to the same level and nature of stress. This observation is not sufficient to explain the apparition of the additional third peak.

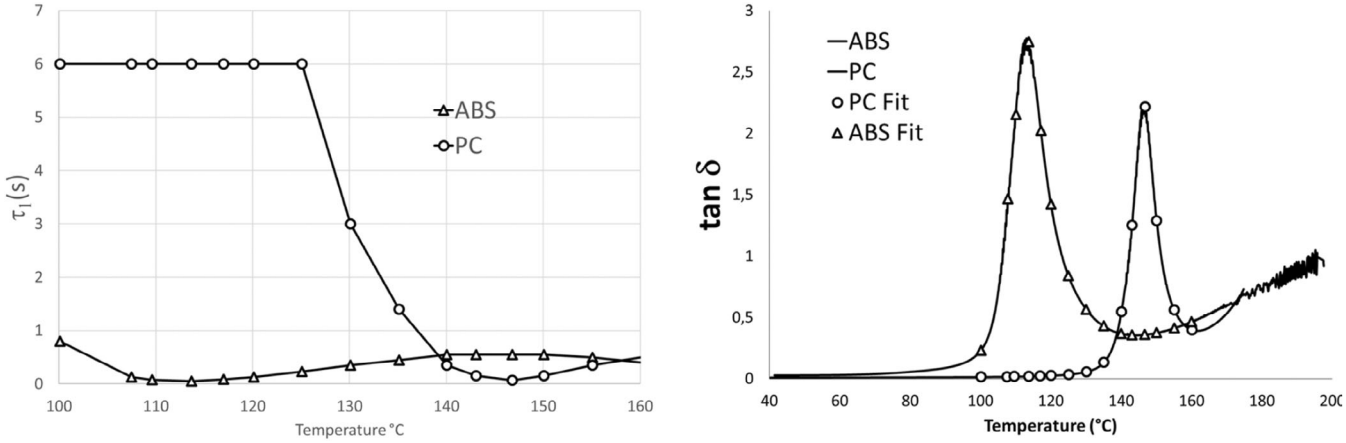

FIGURE 7 Relaxation time versus temperature of virgin polymers acrylonitrile butadiene styrene copolymer (ABS) and polycarbonate (PC)—zoom on temperatures between 100 and 160°C (left) Discrete fitting of $\tan\delta(T)$ of ABS (triangles) and PC (circles) (right)—trend curves (solid line).

3.3 | Discussion

3.3.1 | Predictive simulation with an interphase

To go further, the hypothesis of an interphase between ABS and PC is investigated using the numerical simulation, as Patel et al. have done it for nanocomposites materials.[41] To do so, an interphase with material average properties mainly due to the possible SAN-PC miscibility was considered. An interphase with an arbitrary thickness of 0.4 mm is assumed between ABS and PC considering the partial ABS-PC miscibility of a 25 wt% SAN rate.

The dimensions of the new microstructures are specified in Table 2. As the interphase size has been arbitrarily fixed, a sensitivity analysis is then conducted.

We use the Fox's equation[42] to predict the interphase damping peak $(T_{g\,inter})$from the one of native polymers $(T_{g\,PC}, T_{g\,ABS})$. As we assume miscibility in the interphase area, the interphase damping factor can be deduced from:

$$\frac{1}{T_{g\,inter}} = \frac{\phi_{PC}}{T_{g\,PC}} + \frac{1-\phi_{PC}}{T_{g\,ABS}}. \tag{8}$$

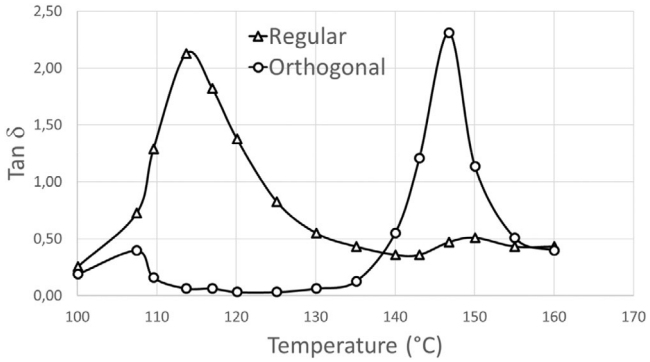

FIGURE 8 Loss factors versus temperature for multilayered structures acrylonitrile butadiene styrene copolymer (ABS)/polycarbonate (PC)/ABS "orthogonal" and "regular"—zoom on temperatures between 100 and 160°C—trend curves (solid line).

$T_{g\,inter}$ was estimated around 123°C.

The same methodology as the one proposed for the virgin polymer is used to define materials properties $(\tau_{inter}, \upsilon_{inter}, G_{inter})$ of this interphase. A set of parameters for this interphase: $G_{0\,inter} = G_{0\,ABS}$, $\upsilon_{inter} = \upsilon_{ABS}$ and τ_{inter} leads to a good representation of the interphase relaxation. This relaxation time of the interphase is presented in Figure 9 (left) in comparison with native polymers. This interphase exhibits a maximum peak in its loss factor at 123°C; below and above this value, the behavior interphase is between native polymers (Figure 9 [right]).

A predictive modeling is conducted using these new microstructures; the geometries and meshes are given in Figure 10 (left); boundary conditions are those described in section 2.3.2.3. Results of the finite element simulations are given in Figure 10 (right) for "orthogonal" and "regular" configurations. For the "orthogonal" sample, the presence of the interphase does not impact the evolution of *tan δ*. For the "regular" configuration, the interphase conducts to an increase of *tan δ* between the damping peaks of ABS and PC. This increase could be related to the additional peak observed in the experimental value obtained for the "regular" multilayered sample (Figure 4). To go further in this analysis, the interphase behavior should be finely characterized with microscopy tools (e.g., AFM for example).

The charge transfer in the multilayered material is very different in the presence of the interface between the two configurations. The average strain components can be numerically evaluated in both situations for each layer component (ABS, PC, and interphase).

An equivalent strain can be computed as follow (Equation 9):

$$\varepsilon_{eq} = \frac{1}{\sqrt{2}}\left[\left(\varepsilon_{xx}-\varepsilon_{yy}\right)^2 + \left(\varepsilon_{yy}-\varepsilon_{zz}\right)^2 + \left(\varepsilon_{zz}-\varepsilon_{xx}\right)^2 + 6\left(\varepsilon_{xy}{}^2 + \varepsilon_{xz}{}^2 + \varepsilon_{yz}{}^2\right)\right]^{1/2}. \tag{9}$$

This equivalent average strain is given in Figure 11 for samples loaded under a temperature of 125°C and for an

TABLE 2 Multilayered dimensions for "orthogonal" and "regular" microstructures ABS/PC/ABS assuming the existence of an interphase. [Color table can be viewed at wileyonlinelibrary.com]

Geometry	ϕ_{PC}%	L (mm)	l (mm)	h (mm)	e (mm)	i (mm)
Orthogonal	33.5	11.88	5.02	3.42	1.48	0.4
Regular	33.3	15.50	3.42	5.02	0.94	0.4

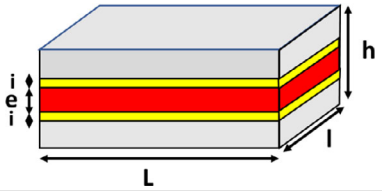

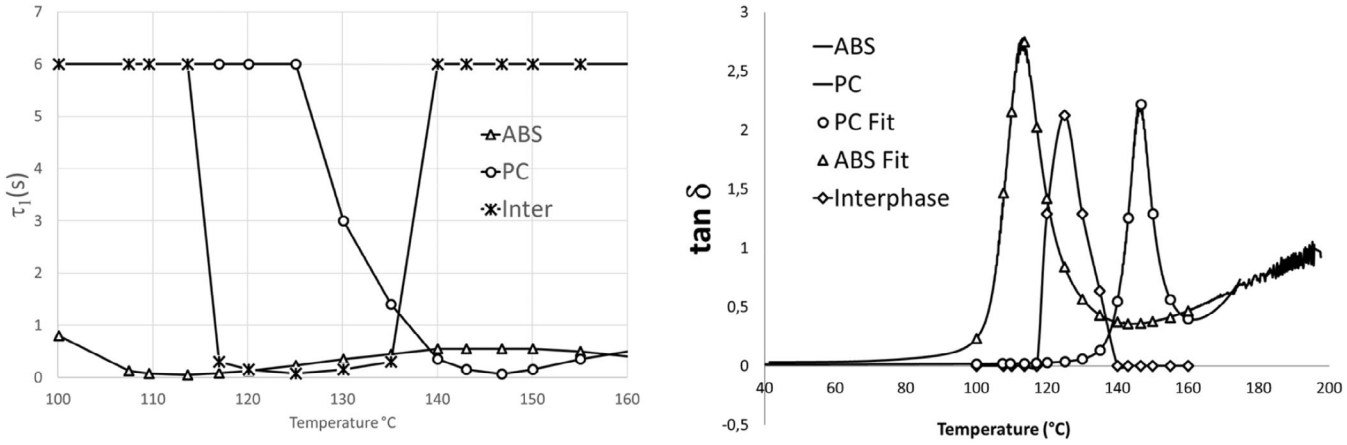

FIGURE 9 Relaxation time versus temperatures of interphase and virgin polymers acrylonitrile butadiene styrene copolymer (ABS), polycarbonate (PC)—zoom on temperatures between 100 and 160°C—trend curves (solid line) (left) evolution of $\tan\delta(T)$ (continuous line) versus time and discrete fiting (diamond) of interphase behavior (right).

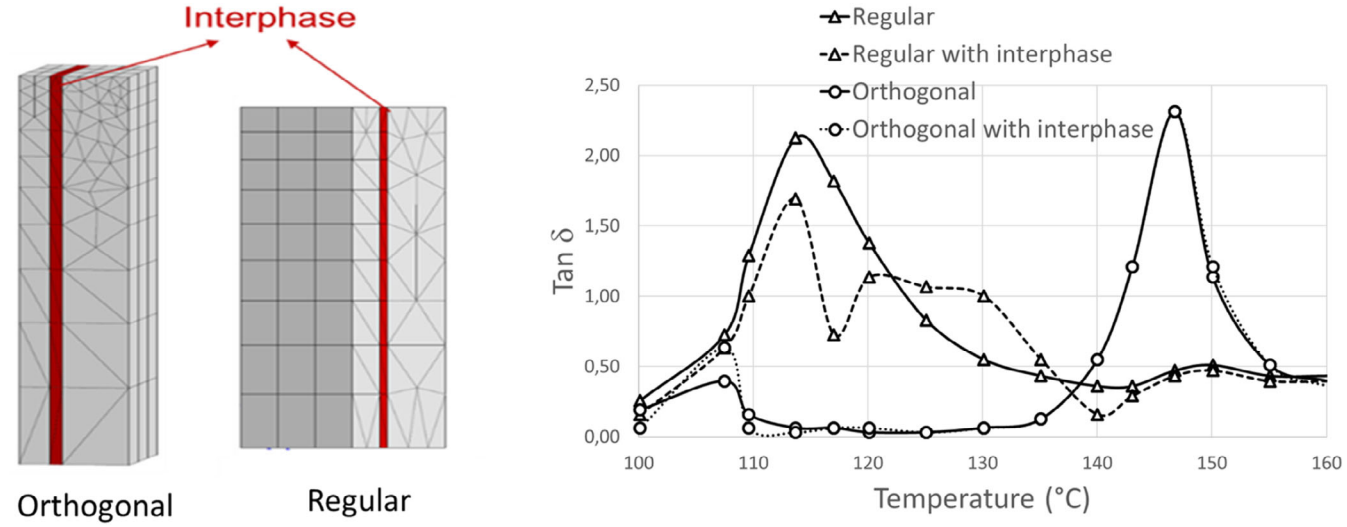

FIGURE 10 FE geometries and meshes for multilayered materials acrylonitrile butadiene styrene copolymer (ABS)/polycarbonate (PC)/ABS with interphase between layers (left) Loss factors versus temperature for multilayared ABS/PC/ABS structures "orthogonal" and "regular" with an interphase of 0.4 mm between the layers—zoom on temperatures between 100 and 160°C (right). [Color figure can be viewed at wileyonlinelibrary.com]

axial strain of 0.04%. It appears that in the "regular" configuration the PC layer is almost not loaded, which leads to a disappearance of its associated peak at 147°C in Figure 10. On the other hand, the interphase in the "regular" configuration exhibits the higher equivalent strain (0.1%), which could explain the increase of the loss damping between the two native peaks of PC and ABS. In the "orthogonal" configuration, the equivalent strain is almost the same for all layers of the components, suggesting that the interphase is not sufficiently stretched to contribute to the loss factor evolution.

3.3.2 | Sensitivity analysis

Further analyzes are needed to properly describe the interphase between layers. Let us first consider the thickness of the interface, value which was fixed a priori in the previous study. As it is shown in Figure 12 (left), decreasing the thickness of the interface leads to lessen the contribution of the interphase (by decreasing the value of tan δ between 120°C and 130°C) to favor that of ABS (at 114°C).

4 | CONCLUSION

Trilayer ABS/PC/ABS films fabricated by thermocompression have been characterized using dynamic mechanical thermal analysis in tensile mode. When the film is loaded in parallel to the layers, an intermediate damping peak is observed in the DMTA curves, while this peak is not present when the film is loaded orthogonally to the layers. Numerical computations show no difference in the behavior of the films in both configurations, suggesting that the origin of the observed intermediate peak is not a purely mechanical phenomenon. However, assuming the presence of an interphase with its own behavior and thickness leads to differences in the local mechanical behavior of the two configurations. Moreover, computations reveal the appearance of an additional peak for the loss factor as the film is loaded in parallel to its layers. The interphase thickness considered in the computations (around 400 μm) seems in reasonable accordance with interphases measured for compatible polymer blends. More experiments are needed to properly quantify and qualify this interphase, but this first study shows clearly the relevance of an interphase. Dynamic tests Charpy, Izod or dynamic traction could confirm this conclusion. Since polycarbonate is more notch sensitive than ABS, the "regular" sample direction should allow more absorption of impact energy (due to the presence extra peak) in comparison with the "orthogonal" one.

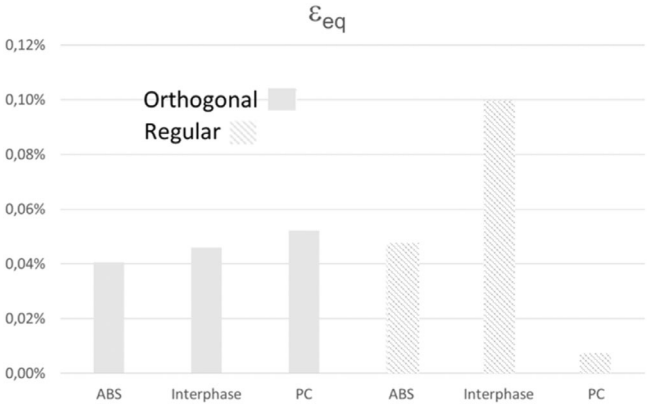

FIGURE 11 Average value of the equivalent strain in each layer of material for "orthogonal" and "regular" acrylonitrile butadiene styrene copolymer (ABS)/polycarbonate (PC)/ABS configuration at 125°C and for an applied axial strain of 4^{e-4}.

AUTHOR CONTRIBUTIONS

Anne-Sophie Caro: Conceptualization (equal); formal analysis (equal); investigation (equal); validation (equal); writing – original draft (lead); writing – review and editing (lead). **Aboubaker Alkhuder:** Data curation (lead); writing – original draft (supporting). **Matthieu Gervais:** Conceptualization (equal); data curation (equal); formal analysis (equal); investigation (equal); project administration (equal); supervision (equal); validation (equal); writing – original draft (supporting); writing – review and editing (supporting). **Alain Guinault:** Project administration (supporting); supervision (supporting). **Patrick Ienny:** Conceptualization (equal); formal analysis (equal); investigation (equal); project administration (equal); supervision (equal); validation (equal); writing – original draft (supporting); writing – review and editing (supporting). **Didier Perrin:** Conceptualization (equal); formal analysis (equal); investigation

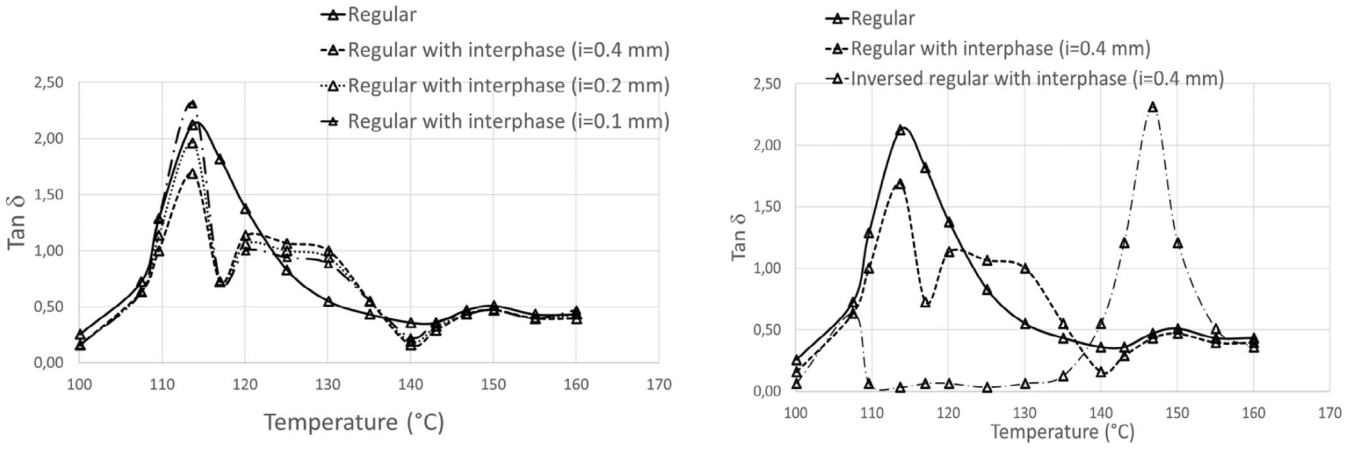

FIGURE 12 Loss factors versus temperature: for "regular" (acrylonitrile butadiene styrene copolymer [ABS]/polycarbonate [PC]/ABS) (left); for "inverse regular" (PC/ABS/PC) multilayered structure with 0.4 mm interphase» (right)—zoom on temperatures between 100 and 160°C.

(equal); project administration (equal); supervision (equal); validation (equal); writing – original draft (supporting); writing – review and editing (supporting). **Cyrille Sollogoub:** Conceptualization (equal); formal analysis (equal); investigation (equal); project administration (equal); supervision (equal); validation (equal); writing – original draft (supporting); writing – review and editing (supporting).

DATA AVAILABILITY STATEMENT

Data are available on request.

ORCID

Anne-Sophie Caro https://orcid.org/0000-0001-7743-1915

REFERENCES

[1] A. Boudenne, L. Ibos, Y. Candau, S. Thomas, *Handbook of Multiphase Polymer Systems*, John Wiley and Sons Ltd, Chichester, Royaume-Uni **2011**.
[2] B. Pukánszky, *Eur. Polym. J.* **2005**, *41*, 645.
[3] A. Zamani Zakaria, K. Shelesh-Nezhad, *Nanomater Nanotechnol.* **2014**, *4*, 4.
[4] G. X. Chen, H. S. Kim, B. H. Park, J. S. Yoon, *Polymer.* **2006**, *47*, 4760.
[5] Y. Zare, K. Y. Rhee, *Eur. Polym. J.* **2017**, *87*, 389.
[6] W. Qi, M. Liu, J. Wu, Q. Xie, L. Chen, X. Yang, B. Shen, X. Bian, W. L. Song, *Compos. Part B Eng.* **2022**, *232*, 109613.
[7] S. Zid, M. Zinet, E. Espuche, *J. Polym. Sci. Part B Polym. Phys.* **2018**, *56*, 621.
[8] X. Colin, G. Teyssèdre, M. Fois, in *Handbook of Multiphase Polymer Systems* (Eds: A. Boudenne, L. Ibos, Y. Candau, S. Thomas), John Wiley, Chichester, Royaume-Uni **2011**, p. 797.
[9] H. Koriyama, H. T. Oyama, T. Ougizawa, T. Inoue, M. Weber, E. Koch, *Copolymer* **1999**, *40*, 6381.
[10] J. Zhang, T. Lodge, C. Macosko, *Macromolecules* **2005**, *38*, 6586.
[11] M. Stamm, D. W. Schubert, *Annu. Rev. Mater. Sci.* **1995**, *25*, 325.
[12] J. Cavaillé, C. Jourdan, J. Perez, *Makromol. Chem. Macromol. Symp.* **1988**, *16*, 341.
[13] J. Cavaillé, J. Perez, *Makromol. Chem. Macromol. Symp.* **1990**, *35*, 405.
[14] T. B. Lewis, L. E. Nielsen, M. Company, *Dynamic Mech. Properties Particulate Filled Compos.* **1970**, *14*, 1449.
[15] H. Eklind, S. Schantz, F. H. J. Maurer, P. Jannasch, W. Bengt, *Macromolecules* **1996**, *29*, 984.
[16] E. P. Douglas, A. J. Waddon, W. J. MacKnight, *Macromolecules* **1994**, *27*, 4344.
[17] E. Girard-Reydet, H. Sautereau, J. P. Pascault, *Polymer* **1999**, *40*, 1677.
[18] H. Eklind, F. H. J. Maurer, *Polymer* **1996**, *37*, 2641.
[19] D. Colombini, F. H. J. Maurer, *Macromolecules* **2002**, *35*, 5891.
[20] B. Gregory, A. Hiltner, E. Baer, J. Im, *Polym. Eng. Sci.* **1987**, *27*, 568.
[21] K. W. McLaughlin, *Polym. Eng. Sci.* **1989**, *29*, 1560.
[22] S. Nazarenko, D. Haderski, A. Hiltner, E. Baer, *Polym. Eng. Sci.* **1995**, *35*, 1682.
[23] A. J. Hsieh, A. W. Gutierrez, *MRS Online Proc. Libr.* **1996**, *461*, 165.
[24] J. Shen, J. Li, S. Guo, *Polymer* **2012**, *53*, 2519.
[25] J. Shen, M. Wang, J. Li, S. Guo, S. Xu, Y. Zhang, T. Li, M. Wen, *Eur. Polym. J.* **2009**, *45*, 3269.
[26] F. Zhang, G. He, K. Xu, H. Wu, S. Guo, *J. Appl. Polym. Sci.* **2015**, *132*, 1.
[27] P. S. Chua, *Polym. Compos.* **1987**, *8*, 308.
[28] F. Zhang, M. Guo, K. Xu, G. He, H. Wu, S. Guo, *Compos. Sci. Technol.* **2014**, *101*, 167.
[29] R. Greco, *Polym. Blends Alloys*, CRC Press, Boca Raton **2019**.
[30] G. Roberto, A. Sorrentino, *Adv. Polym. Technol.* **1994**, *13*, 249.
[31] H. Suarez, J. Barlow, D. Paul, *J. Appl. Polym. Sci.* **1984**, *29*, 3253.
[32] A. Guinault, C. Sollogoub, *Int. J. Mater. Form.* **2009**, *2*, 701.
[33] J. D. Keitz, J. W. Barlow, D. R. Paul, *J. Appl. Polym. Sci.* **1984**, *29*, 3131.
[34] F. Carrasco, O. Santana, J. Cailloux, M. Sanchez-Soto, M. L. Maspoch, *Polym. Test.* **2018**, *67*, 468.
[35] W. N. Kim, C. M. Burns, *J. Appl. Polym. Sci.* **1990**, *41*, 1575.
[36] S. Aid, A. Eddhahak, Z. Ortega, D. Froelich, A. Tcharkhtchi, *J. Appl. Polym. Sci.* **2017**, *134*, 44975.
[37] J. Besson, R. Leriche, R. Foerch, G. Cailletaud, *Rev. Eur. Des. Éléments Finis.* **1998**, *7*, 567.
[38] M. Akay, S. Ozden, *Plast. Rubber Compos. Process. Appl.* **1996**, *25*, 138.
[39] S. Pandini, A. Pegoretti, *Express Polym. Lett.* **2011**, *5*, 685.
[40] L. Yang, L. Yang, R. L. Lowe, *Mech. Mater.* **2020**, *2021*, 103839.
[41] R. K. Patel, B. Bhattacharya, S. Basu, *Mech. Res. Commun.* **2008**, *35*, 115.
[42] T. G. Fox, *Bull. Am. Phys. Soc.* **1956**, *1*, 123.